JOURNAL OF MATERIALS SCIENCE 22 (1987) 2847–2851

Oxygen evolution during the formation and sintering of nickel–manganese oxide spinels for thermistor applications

F. GOLESTANI-FARD, S. AZIMI
Materials and Energy Research Centre, PO Box 14155-4777, Tehran, Iran
K. J. D. MACKENZIE
Chemistry Division, DSIR, Private Bag, Petone, New Zealand

Nickel–manganese spinel, prepared from 20 wt% NiO and 80 wt% Mn_2O_3, forms at 950° C by the intermediate formation of Mn_3O_4 with evolution of oxygen, determined by mass-spectrometric evolved gas analysis. On heating to higher temperatures, further oxygen is evolved resulting in pore formation and bloating of pressed sintered samples and anomalies in their densification and electrical properties. Thermodynamic considerations and X-ray diffraction intensity measurements suggest that all the Mn^{2+} is located in the tetrahedral spinel sites, this cation configuration remaining unchanged by higher-temperature treatments such as sintering.

1. Introduction

Negative-temperature coefficient (NTC) thermistors are thermally-sensitive resistors whose resistance decreases with increasing temperature [1, 2]. Since NTC thermistor materials are generally mixed-oxide compounds [3, 4], the electrical properties of a number of mixed-oxide systems, including nickel–manganese oxides, have been investigated for this application [5, 6]. NTC thermistor materials based on nickel–manganese oxides of composition $Ni_{1-x}Mn_{2+x}O_4$ have been found to adopt the spinel structure where $x < 0.4$; such compounds exhibit n-type semiconductivity, and for practical applications their resistivity can be decreased by doping with Cu^{2+} [7].

In a recent microstructural study of nickel–manganese oxide thermistors containing 1% CuO [8], anomalous sintering and electrical behaviour was observed which was thought to be due to oxygen evolution during firing. The present work addresses this question by studying the formation of nickel–manganese oxide without CuO additions, using thermal analysis, evolved gas analysis (EGA), X-ray and microstructural techniques and electrical measurements.

2. Experimental procedure

An intimate mixture of 20 wt % NiO and 80 wt % Mn_2O_3 was obtained by heating MnO_2 at 700° C for 4 h; the resulting weight loss of 9.5% is in good agreement with the theoretical weight loss for complete formation of Mn_2O_3 (9.2%). The oxide mixture was converted to nickel–manganese oxide by firing in air for 8 h at 950° C. Thermal analysis was carried out both on the unfired mixture and the material produced at 950° C, using a Netzsch model 404 differential thermal analyser and a Stanton Redcroft model TG770 thermobalance at a heating rate of $10° C\,min^{-1}$ in a dynamic air atmosphere. EGA were made using a quadrupole mass spectrometer (Extranuclear Corp.) with argon as the carrier gas. Unit-cell dimensions of all the products were measured using a computer-controlled Philips PW 1700 X-ray diffractometer with Co$K\alpha$ radiation and a graphite monochromator. The internal angular calibrant was silicon.

The product fired at 950° C was pelletized at $3.5 \times 10^3\,kg\,cm^{-2}$ and sintered in air at various temperatures up to 1350° C, the process being monitored by measurements of bulk density and room temperature electrical resistivity. The experimental details of these measurements are given elsewhere [8]. Scanning electron microscopy was carried out on the sintered pellets using a Cambridge electron microscope.

3. Results and discussion

The thermal analysis curves for the unreacted oxide mixture are shown in Fig. 1. Two small endothermic events at about 300 and 600° C accompanied by a total weight loss of 0.5%, are seen from the corresponding mass 44 EGA signal to be due to the decomposition of carbonate. Carbonate impurities may be present both in nickel oxide, and, as a result of recarbonation, in the manganese oxide; the temperatures of these two events correspond well with the reported decomposition temperatures of nickel and manganese carbonates (about 375 and 600° C respectively [9]). The higher-temperature weight-loss (Fig. 1A) can be seen by differential thermal analysis (DTA) and derivative thermogravity (DTG) to be a double event, both stages of which involve the loss of oxygen only (Fig. 1D). (The apparent discrepancy between the temperatures of the EGA experiment and the other thermal analysis curves is probably due to the inert

0022–2461/87 $03.00 + .12

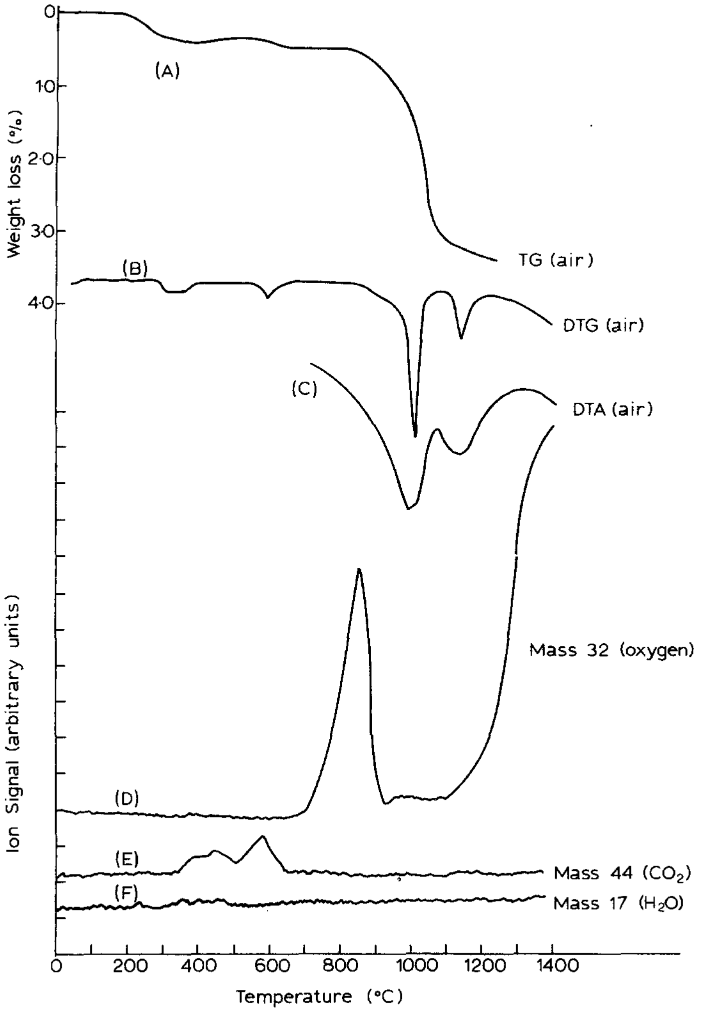

Figure 1 Thermal analysis and EGA curves for 20 wt % NiO + 80 wt % Mn_2O_3 mixture. Heating rate 10° min^{-1}.

atmosphere used in the EGA experiments). These oxygen losses are related to the thermal decomposition behaviour of the manganese oxides themselves, which, when heated alone under oxidizing conditions, pass through a series of increasingly oxygen-deficient compositions, including some of variable stoichiometry [10]. Thus, at about 1000° C Mn_2O_3 is converted to Mn_3O_4, with a theoretical weight loss of 3.4% (since in the present samples only 80% is Mn_2O_3, the theoretical weight loss for its conversion to Mn_3O_4 is 2.7%, in good agreement with the observed 2.6% loss up to 1080° C). This decomposition is accompanied by the formation of nickel–manganese spinel, possibly facilitated by the appearance of divalent ions in the Mn_3O_4 structure, with which Ni^{2+} can exchange. Nickel oxide was found to react even more readily and completely with Mn_3O_4 prepared from MnO_2 by prefiring at 950° C. In inert atmospheres, the decomposition of Mn_2O_3 to Mn_3O_4 occurs $\sim$200° C lower than in oxidizing conditions [10], explaining the displacement of the oxygen evolution peak to 850° C under the argon atmosphere of the EGA experiment.

The continuous loss of further oxygen on heating to $> 1120°$ C has also been reported in Mn_3O_4 [10], which in air becomes slightly oxygen deficient, forming Mn_3O_{3+x}, but under inert conditions is gradually reduced to MnO with increasing temperature [10]. The nickel–manganese oxide apparently behaves similarly, since oxygen evolution at higher temperatures was found even in mixtures in which $NiMn_2O_4$ had previously been formed by firing at 950° C for 8 hours (Fig.2).

In this case, the thermal events and oxygen evolution associated with the formation of Mn_3O_4 are absent, this reaction having occurred during the initial firing, but a 0.65 wt % oxygen loss is again found at $> 1080°$ C, in good agreement with the 0.7% oxygen loss found in this temperature range in samples not pre-reacted (Fig. 1). This weight loss corresponds to the further loss of 0.1 oxygen atom per mole of spinel, and may result from the conversion of a similar amount of Mn^{3+} to Mn^{2+}. Attempts to confirm this point by EPR spectroscopy were unsuccessful.

Another interesting point emerges from Fig. 2; on prolonged standing in the ambient atmosphere, the product formed at 950° C undergoes significant recarbonation, as seen from the CO_2 evolution curve from this material (Fig. 2D). No unreacted manganese oxides are detectable in this material by X-ray diffraction, the only phases present being the spinel and a small amount of unreacted NiO, and since the temperature of the principal decarboxylation peak is more typical of manganese than nickel carbonate, it might be inferred that when formed at this temperature, the spinel itself is capable of significant recarbonation, possibly reflecting its manganese-rich composition. The high-temperature evolution of oxygen from this ferrite has practical consequences for its fabrication behaviour and its physical and electrical properties as

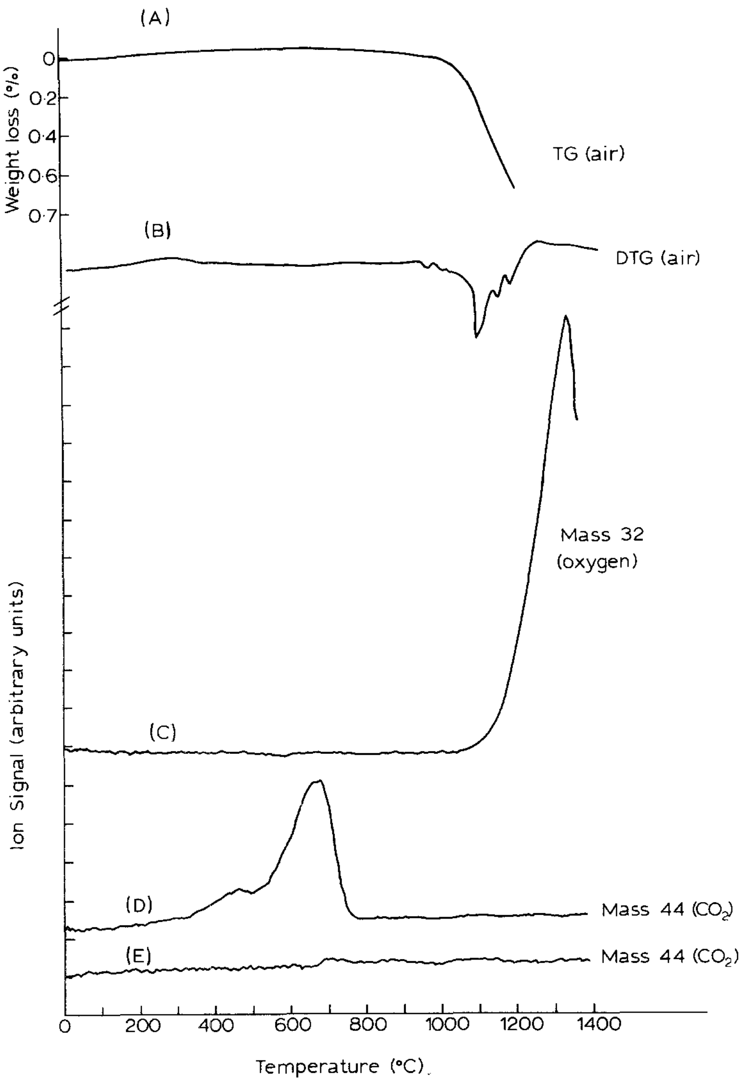

Figure 2 Thermal analysis and EGA curves for 20 wt % NiO + 80 wt % Mn_2O_3 pre-fired at 950° C for 8 h to form nickel-manganese spinel. (E) CO_2 evolution from freshly-prepared spinel, (D) CO_2 evolution from spinel after prolonged standing in air.

an NTC thermistor material, since pellets pressed from the spinel pre-formed at 950° C evolve further oxygen during sintering, causing them to bloat and develop pores and blowholes (Fig. 3).

The effects of this porosity on the density and electrical resistivity are shown in Fig. 4, which indicates that sintering at $> 1100°$ C produces a decrease in the bulk density and an increase in the room-temperature resistivity. Similar sintering behaviour observed in nickel–manganese oxides doped with CuO [8] was found not to be caused by phase changes occurring during the firing process, but in the light of the present results, is probably also caused by oxygen evolution during sintering.

3.1. The possible constitution of the present spinel

On the basis of the thermal analysis results and the composition of the mixture of starting oxides, the present spinel appears to be based on Mn_3O_4, i.e. it

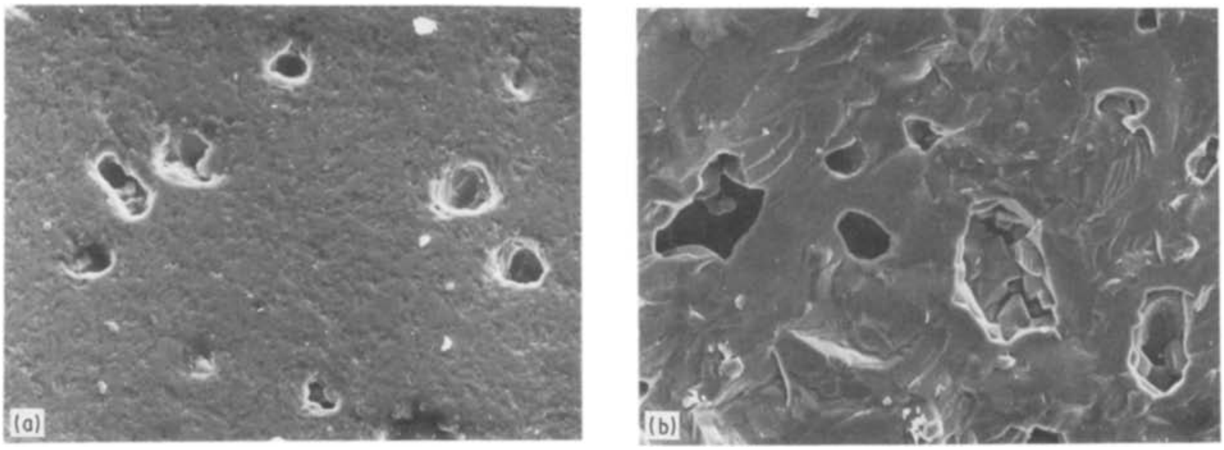

Figure 3 Scanning electron micrographs of pressed nickel–manganese spinel pellets sintered in air at 1300° C for 4 h × 910. (a) pellet surface, as pressed, (b) fractured surface.

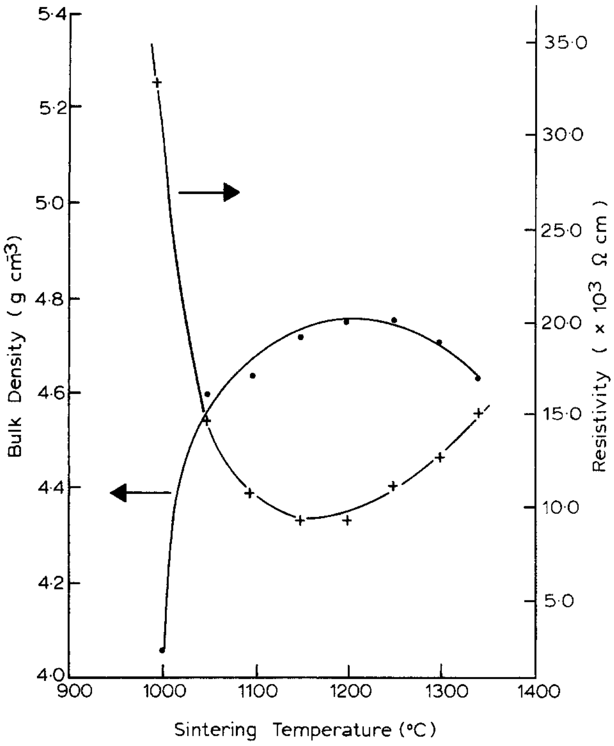

Figure 4 Bulk density and room-temperature electrical resistivity of nickel–manganese spinel pellets as a function of sintering temperature. Sintering time 4 h.

contains both Mn^{2+} and Mn^{3+}. In terms of a starting composition of 0.27 mol of NiO and 0.34 mol of Mn_3O_4, and normalizing to a four-oxygen cell, the formula would be

$$Ni^{2+}_{0.66}Mn^{2+}_{0.83}Mn^{3+}_{1.66}O_4$$

Since the total cation charge of this formulation is slightly too high, it might be compensated for by a slight change in the oxygen stoichiometry. From thermodynamic considerations [11], Mn^{2+} has a significant preference for tetrahedral sites in spinels, whereas both Ni^{2+} and Mn^{3+} have octahedral site preferences, that of Mn^{3+} being stronger than Ni^{2+}. On this basis, the spinel formed at 950° C might be written

$$(Mn^{2+}_{0.83}Ni^{2+}_{0.17})\ [Mn^{3+}_{1.66}Ni^{2+}_{0.49}]\ O_4 \qquad \text{(structure A)}$$

The octahedral cations are contained in the square brackets.

An independent method of establishing the constitution of this spinel is suggested by the work of Boucher *et al.* [12] which reports a linear relationship between the degree of inversion V of the spinel and its lattice parameter a:

$$a = 8.441 - 0.057V \qquad (1)$$

Extrapolating this relationship to the measured a-values of the present spinels formed at 950° C (0.8426 – 0.8429 nm) indicates inversion parameters of 0.21–0.26, i.e. all the available nickel would be in the tetrahedral sites. Since only 0.66 gm atoms of nickel are available, the formulation on this basis would be

$$(Mn^{2+}_{0.34}Ni^{2+}_{0.66})\ [Mn^{3+}_{1.66}Mn^{2+}_{0.54}]\ O_4 \qquad \text{(structure B)}$$

To check which of these models is more correct, the X-ray diffraction intensities from the various crystallographic planes of the spinel were calculated for the two structures, and compared with the observed integrated intensities, which are a function of the distribution of nickel and manganese cations over the available tetrahedral and octahedral sites.

Assuming random orientation, the intensity of any $h\,k\,l$ reflection (I_{hkl}) is given by

$$I_{hkl} = |F|^2_{hkl}P_{hkl}(1 + \cos^2 2\theta/\sin^2\theta\cos\theta)_{hkl} \qquad (2)$$

where $|F|$ is the structure factor, P is the multiplicity factor (to correct for the superposition of diffracted beams from several planes) and the term containing the Bragg angle θ is the Lorentz-polarization factor. The structure factor is a function of the number and distribution of the atoms in the diffracting plane, and their atomic scattering factors, which are related to their atomic mass.

Following Datta and Roy [13], intensity calculations were made for the 4 0 0 and 4 2 2 reflections of the spinel structures A and B. The choice of these reflections follows the suggestion of Durif-Varambon *et al.* [14] that the ratio of these intensities is a diagnostic indicator of cation distributions in the spinel structure. In view of the similarity of the atomic scattering factors for Mn^{2+} and Mn^{3+}, the valency of the manganese was not distinguished, a mean manganese scattering factor being assumed.

Comparison of the calculated intensity ratios I_{400}/I_{422} for structures A and B (3.25 and 2.06, respectively) with the measured integrated intensity ratios for samples prepared at 950° C (2.74–3.04) suggests that the model derived from thermodynamic considerations is the more correct; extrapolation of the linear relationship of Boucher *et al.* [12] for spinels of larger a-parameter is apparently not valid.

Heat treatment of these spinels at 1250° C has a variable effect on the a-parameter, which in one case increased to 0.8447 nm but in another case remained unchanged. By contrast, the intensity ratios I_{400}/I_{422} (2.64–2.73) were relatively uninfluenced by heat treatment, suggesting that although heating may cause changes in the oxygen packing, the cation distribution within this oxygen lattice remains relatively stable.

4. Conclusions

1. NTC thermistor materials prepared from mixtures of 20 wt % NiO and 80 wt % of Mn_2O_3 form a spinel phase at 950° C by initial formation of Mn_3O_4 with the evolution of oxygen. The appearance of some Mn^{2+} probably facilitates the diffusion of Ni^{2+} into the structure.

2. On further heating, the spinel continues to lose small but significant amounts of oxygen, behaving similarly to the Mn_3O_4 on which it is based. This oxygen evolution results in pore formation and bloating in pressed sintered samples, and is responsible for anomalies in the densification and electrical properties of the sintered compacts.

3. Thermodynamic considerations suggest that all the Mn^{2+} is located in the tetrahedral sites of the spinel, the balance being Ni^{2+}, most of which is how-

ever located with the Mn^{3+} in the octahedral sites. This structural model is supported by calculations of X-ray diffraction intensities. Extrapolation of structural information from cell-parameter data appears not to be valid, giving results which are consistent neither with thermodynamic considerations, nor with intensity calculations.

Acknowledgements

We are indebted to Dr I. W. M. Brown for the X-ray measurements, to Mrs L. M. Parker and N. J. Tapp for the thermal analysis and EGA experiments, to Mrs K. Card for the scanning electron microscopy, and to Dr T. Hashemi, Materials and Energy Research Centre, for helpful discussion.

References

1. J. A. BECKER, C. B. GREEN and G. L. PEARSON, *Eng. Trans.* **65** (1946) 711.
2. E. D. MACKLEN, "Thermistors", (Electrochemical Publications Ltd, Ayr, Scotland, 1979).
3. Standard Telephones and Cables Ltd and E. F. Dearborn, Brit. Patent 540 844, "Resistance Materials and Methods of Making the Same", (1941).
4. D. W. JOHNSON Jr, N. ROBBINS, E. M. VOGEL and V. G. LAMBRECHT Jr, *Amer. Ceram. Soc. Bull.* **62** (1983) 597.
5. R. W. A. SCARR and R. A. SETTERINGTON, *IEE Paper No. 3176M* (1960) 395.
6. H. B. SACHSE, in "Semiconducting Temperature Sensors and their Application", (Wiley, New York, 1975).
7. T. HATA, T. KURODA and Y. MATSUO, *Natl. Tech. Rept.* **28** (Matsushita Elec. Ind. Co., Osaka, Japan, 1982) 1123.
8. S. AZIMI, F. GOLESTANI-FARD and T. HASHEMI, in Proceedings of the 6th CIMTEC Congress on Hi-Tech. Ceramics, Faenza, Italy (1986).
9. R. C. MACKENZIE (ed.) "The Differential Thermal Investigation of Clays" (Mineralogical Society, London, 1957) Ch. 13.
10. K. J. D. MACKENZIE, *Rev. Anal. Chem.* **7** (1983) 193.
11. A. NAVROTSKY and O. J. KLEPPA, *J. Inorg. Nucl. Chem.* **29** (1967) 2701.
12. B. BOUCHER, R. BUHL and M. PERRIN, *Acta Cryst.* **B25** (1969) 2326.
13. R. K. DATTA and R. ROY, *J. Amer. Ceram. Soc.* **50** (1967) 578.
14. A. DURIF-VARAMBON, E. F. BERTAUT and R. PAUTHENET, *Ann. Chim. (Paris)* **1** (1956) 525.

Received 17 September
and accepted 8 December 1986